Effects of Monocular Deprivation and Reverse Suture On Orientation Maps Can Be Explained By Activity-Instructed Development of Geniculocortical Connections

Kenneth D. Miller[†] **and Ed Erwin**[*]
Depts. of Physiology[*,†] and Otolaryngology[†],
W.M. Keck Center for Integrative Neuroscience[*,†],
Sloan-Swartz Center for Theoretical Neurobiology[†]
University of California
San Francisco, CA 94143-0444
ken@phy.ucsf.edu, erwin@phy.ucsf.edu

In Press, Visual Neuroscience — Aug. 15, 2001

Abbreviated title: Monocular Deprivation and Reverse Suture
Text data: 34 text pages, 0 tables, 8 figures.

Address Correspondence To:
Kenneth Miller
Dept. of Physiology
UCSF
513 Parnassus
SF, CA 94143-0444
Phone: 415-476-8217
Fax: 415-476-4929
email: ken@phy.ucsf.edu

Abstract

Mature visual cortex shows a single, binocularly matched orientation map. This matching develops without visual experience. It persists despite early monocular deprivation that largely eliminates one eye's map, followed by reverse suture (deprivation of the previously open eye and opening of the previously deprived eye), even though the two eyes lack common visual experience in this case. These results have been interpreted to suggest that the structure of orientation maps either is innately predetermined or, if it arises through self-organization, is determined by external cues such as boundary conditions or a "scaffolding" of horizontal connections. We show, to the contrary, that these results are the expected outcomes if orientation maps develop through activity-instructed, correlation-based development of the geniculocortical connections without additional cues. A weak, binocularly correlated orientation map is known to exist before deprivation onset; we previously showed how this can arise through activity-instructed development. Now we show that this initial correlation between the two eyes' maps can persist or increase despite deprivation sufficient to cause massive loss of the deprived eye's geniculocortical synaptic strength, followed by reverse suture. Given sufficient early correlated map development, each map's fate is "dynamically committed": the two eyes' maps will converge upon a common outcome, even if developing independently. This dynamic fate commitment is retained even after severe deprivation.

Keywords: Hebb synapse, visual cortex, striate cortex, simple cell, binocular cell, monocular deprivation, V1

A central problem in neuroscience is to understand the formation of cerebral cortical maps. Much evidence suggests a role of neuronal activity in instructing the development of ocular dominance maps (Katz & Shatz, 1996; Stryker & Harris, 1986; Stryker & Strickland, 1984; but see Crowley & Katz, 1999, 2000) and the maturation of orientation selectivity (Chapman & Stryker, 1993; Crair et al., 1998; Fregnac & Imbert, 1984; Weliky & Katz, 1997). Recent results show that the initial development of orientation selectivity also depends on patterns of input activity (Chapman & Gödecke, 2000). Nonetheless the role of activity in the initial design of orientation maps remains controversial. Orientation selectivity arises early in development, before eye-opening in kittens (*e.g.*, Albus & Wolf, 1984; Braastad & Heggelund, 1985; Hubel & Wiesel, 1963) and ferrets (Chapman & Stryker, 1993) and before birth in monkeys (Wiesel & Hubel, 1974), and the initial development of orientation maps does not depend on visual experience (Chapman et al., 1996; Crair et al., 1998; Wiesel & Hubel, 1974). Thus, any activity-dependence in the initial development of orientation selectivity and maps must involve dependence on spontaneous rather than visually-driven activity.

A challenge to the hypothesis of activity-instructed orientation map development was posed by studies of the effects of monocular deprivation and reverse suture on the ocular matching of cat orientation maps (Gödecke & Bonhoeffer, 1996). In this paradigm, one eyelid was kept shut from birth until P35 (postnatal day 35). This deprivation largely, though not entirely (Antonini et al., 1998; Crair et al., 1997), eliminated the deprived eye's orientation map, while the open eye's map remained normal. The initial deprivation was followed by reverse suture — closing of the previously open eye, and opening of the previously closed eye — at a time (P35) when this can still reverse the effects of the initial deprivation. After enough time to restore connections from the newly-opened eye, its orientation map was measured and found to match the map recorded previously in the originally-open eye, even though the two eyes had never had common visual experience.

These results were argued to require that the preferred orientations of cortical cells, if determined by the organization of geniculocortical connections (as appears to be the case for simple cells in layer 4 of cat V1, *e.g.* Ferster et al., 1996; Ferster & Miller, 2000; Reid & Alonso, 1995), must be "innately" specified, rather than "acquired" in an activity-instructed manner (Gödecke & Bonhoeffer, 1996). This inference depends on the assumption that the deprivation obliterated any residue of the orientation map in the deprived-eye's geniculocortical connections. Alternatively, it was argued, the map may develop in an activity-dependent manner but with its structure specified by factors other than the organization of geniculocortical connections. Modelers have examined several possible factors, arguing that orientation maps may be determined by cortical boundary conditions (Wolf et al., 1996) or by horizontal intracortical connections (Bartsch & van Hemmen, 2001; Ernst et al., 2001; Shouval et al., 2000), factors that would provide a common influence to each eye's developing map.

Here we show that the results of Godecke and Bonhoeffer (1996) actually follow robustly from the hypothesis of development via activity-instructed plasticity of geniculocortical connections, without requiring any preexisting scaffolding or boundary conditions. Even after severe deprivation, the geniculocortical connections retain sufficient information to largely determine the final orientation map. We assume that weak, binocularly correlated orientation maps have developed in the two eyes before deprivation begins to alter development. Experimentally, this is well supported by the finding that binocularly correlated orientation maps are visible in cats as early as P12 (Crair et al., 1998), a full week before the onset of the critical period for deprivation effects (Fregnac & Imbert, 1984; Movshon & Van Sluyters, 1981; Shatz & Stryker, 1978), and a full week before the presence or absence of visual experience has any detectable effect on development of orientation selectivity or other visual cortical response properties (Crair et al., 1998; Fregnac & Imbert, 1984). We previously showed how such binocularly correlated maps can develop, without need of vision, through appropriate patterns of spontaneous neuronal activity (Erwin & Miller, 1998) We also showed that, given sufficient early correlated map development, each map's fate is "dynamically committed": the two eyes' maps will converge upon a common outcome, even if developing independently. We now show that this dynamic fate commitment can be retained even after severe deprivation sufficient to cause massive loss of synaptic strength. The weak synaptic structure remaining in the deprived eye's projection is sufficient, after reverse suture, to robustly bias development back along the same trajectory as was followed prior to deprivation. This causes the newly opened eye to arrive at an orientation map well-correlated with that observed in the originally opened eye.

An abstract of this work has been presented previously (Erwin & Miller, 1996).

Methods

Model System

Place Fig. 1 about here

We use the model system described in Erwin and Miller (1998), shown in Fig. 1. Briefly: Model cortical cells are arranged in a 32×32 grid with positions denoted by Roman letters, *e.g.* $\vec{x}$ or $\vec{y}$. Model LGN cells are arranged in a corresponding 32×32 grid, with positions denoted by Greek letters, *e.g.* $\vec{\alpha}$ or $\vec{\beta}$. For each LGN position, there are four cell types, representing two eyes (left, L, and right, R) and two center-types (ON-center, N, and OFF-center, F). Hence, the four cell types can be labelled LN, LF, RN, RF.

Connectivity from LGN to cortex is modeled by a static arbor function, $A(\vec{x}, \vec{\alpha})$, and an evolving synaptic weight function, $S(\vec{x}, \vec{\alpha})$. The arbor function, $A(\vec{x}, \vec{\alpha})$, models prior biases in connectivity that are not instructed by activity, *e.g.* the retinotopically allowed range of cortex over which an LGN afferent may arborize or sprout. The synaptic weight variables, $S^{\mathcal{E}\mathcal{C}}(\vec{x}, \vec{\alpha})$, represent the total efficacy or strength of the synaptic connections from LGN cells at position $\vec{\alpha}$ in eye-layer $\mathcal{E} \in \{L, R\}$ and of center type $\mathcal{C} \in \{N, F\}$ to cells at cortical position $\vec{x}$, Fig. 1. This efficacy is necessarily zero where $A(\vec{x}, \vec{\alpha})$ is zero. The spatial receptive field of the cortical cell at $\vec{x}$ is determined by its pattern of geniculate input, represented by $S^{\mathcal{E}\mathcal{C}}(\vec{x}, \vec{\alpha})$.

The dynamic variables in the model are the geniculocortical synaptic weights, $S^{\mathcal{E}\mathcal{C}}$, which define the cortical spatial receptive fields. These weights develop over time under "correlation-based" rules of synaptic development (Miller, 1996a, 1998; Miller et al., 1989). These are rules representing simple firing-rate-based models of a class of underlying mechanisms. These mechanisms have in common the dependence of a structure's development on the correlations among the activities of its inputs: loosely, these are rules that lead to the outcome "neurons that fire together, wire together". These mechanisms include simple versions of Hebbian synaptic modification, activity-dependent release and uptake of diffusible modifying factors, or synaptic sprouting and retraction with activity-dependent stabilization.

To these rules are added constraints, of two types. First, individual weights are constrained to remain non-negative and less than some maximal value. Second, a competitive mechanism must be included to model the fact that different correlated input patterns compete with one another, so that a single correlated pattern of inputs ultimately comes to dominate the receptive field of a given cell (Bienenstock et al., 1982; Guillery, 1972; Miller, 1996b; Miller & MacKay, 1994; Stryker & Strickland, 1984; von der Malsburg, 1973). We enforce competition by conserving the total synaptic strength onto each postsynaptic cell, so that when some inputs onto a cell become stronger others must grow correspondingly weaker. This is meant to model the fact of competition, but not its mechanism, about which little has been known until recently (though see Davis & Goodman, 1998; Song et al., 2000; Turrigiano et al., 1998; Turrigiano & Nelson, 2000).

With simplifying assumptions, simple linear equations describing the evolution of the geniculocortical weights $S(\vec{x},\vec{\alpha})$ can be developed (Miller, 1990). These equations are expressed in terms of three functions. One, the arbor function $A(\vec{x},\vec{\alpha})$, was described above. A second is the set of correlation functions, $C^{\mathcal{E}\mathcal{C},\mathcal{E}'\mathcal{C}'}(\vec{\alpha},\vec{\beta})$, describing the correlation in spiking activity between an input of eye $\mathcal{E}$ and center type $\mathcal{C}$ at position $\vec{\alpha}$, and one of eye $\mathcal{E}'$ and center type $\mathcal{C}'$ at position $\vec{\beta}$ ($\mathcal{E},\mathcal{E}' \in \{L,R\}$; $\mathcal{C},\mathcal{C}' \in \{N,F\}$). The third is the intracortical interaction function, $I(\vec{x},\vec{y})$, describing how active synapses at $\vec{x}$ in cortex influence the growth of coactive synapses at $\vec{y}$. This function summarizes influences due to intracortical connectivity or diffusion of modification factors.

Developmental Equations and Simulation Methods

The equations studied are exactly as in Erwin and Miller (1998), with one exception, described below. For completeness, we list the basic equations here; see the previous paper for full equations along with discussion of their meaning and origins.

Constrained development under a Hebbian or other correlation-based synaptic modification rule takes the form

$$\frac{d}{dt}S^{\mathcal{E}\mathcal{C}}(\vec{x},\vec{\alpha},t) = \begin{cases} \mathcal{H}^{\mathcal{E}\mathcal{C}}[\mathbf{S}](\vec{x},\vec{\alpha},t) - \epsilon(\vec{x},t)A(\vec{x},\vec{\alpha}), & \text{for } \{(\mathcal{E},\mathcal{C},\vec{\alpha})\} \in \mathcal{P}(\vec{x},t), \\ 0, & \text{otherwise.} \end{cases} \quad (1)$$

Here, $\mathbf{S}$ represents the set of all synaptic weights, η is a constant learning rate, $\mathcal{P}(\vec{x},t)$ represents the set of all weights onto the cortical cell at $\vec{x}$ that are considered "plastic," and

$$\mathcal{H}^{\mathcal{EC}}[\mathbf{S}](\vec{x},\vec{\alpha},t) = \eta A(\vec{x},\vec{\alpha}) \sum_{\vec{y}} I(\vec{x},\vec{y}) \sum_{\vec{\beta},\mathcal{E}',\mathcal{C}'} C^{\mathcal{EC},\mathcal{E}'\mathcal{C}'}(\vec{\alpha},\vec{\beta}) S^{\mathcal{E}'\mathcal{C}'}(\vec{y},\vec{\beta},t) \tag{2}$$

represents the unconstrained Hebbian rule. The term $-\epsilon(\vec{x},t)A(\vec{x},\vec{\alpha})$ adds a constraint to the Hebbian dynamics: the value of $\epsilon(\vec{x},t)$ is chosen at each time step to ensure that the total synaptic weight received by each cortical cell remains constant. This represents the fact that the dynamics are competitive, so that when some synapses grow stronger, others must correspondingly weaken.

Synaptic weights are also constrained to remain positive and bounded:

$$0 \leq S^{\mathcal{EC}}(\vec{x},\vec{\alpha}) \leq 8A(\vec{x},\vec{\alpha}), \text{ for all } \mathcal{E},\mathcal{C},\vec{x},\vec{\alpha}. \tag{3}$$

When a synapse reaches its upper or lower limit, we say that it is saturated.

In the previous paper, we allowed plasticity only in synapses that were not saturated. Now, our definition of the set of plastic synapses will be expanded; this is the only difference in equations from the previous paper. Because we are now modeling deprivation and reverse suture, the correlation functions are drastically changed in mid-development (both at onset of deprivation, and onset of reverse suture). Thus, the Hebbian term $\mathcal{H}$ may reverse sign, whereas previously this essentially never occurred for a saturated synapse. Therefore, we now allow plasticity in any saturated synapse when the Hebbian term acts to move it away from a saturation boundary. For example, connections that were reduced to zero during deprivation of one eye's inputs can re-gain strength when input is restored to that eye. Thus, we now define the set of plastic synapses, $\mathcal{P}(\vec{x},t)$, as follows (compare Eq. 6 of Erwin and Miller, 1998):

$$\mathcal{P}(\vec{x},t) = \left\{ (\mathcal{E},\mathcal{C},\vec{\alpha}); \begin{array}{rl} \text{where} & 0 < S^{\mathcal{EC}}(\vec{x},\vec{\alpha},t) < 8A(\vec{x},\vec{\alpha}), \\ \text{or} & S^{\mathcal{EC}}(\vec{x},\vec{\alpha},t) = 0 \text{ and } \mathcal{H}^{\mathcal{EC}}[\mathbf{S}](\vec{x},\vec{\alpha},t) > 0, \\ \text{or} & S^{\mathcal{EC}}(\vec{x},\vec{\alpha},t) = 8A(\vec{x},\vec{\alpha}) \text{ and } \mathcal{H}^{\mathcal{EC}}[\mathbf{S}](\vec{x},\vec{\alpha},t) < 0 \end{array} \right\}. \tag{4}$$

Our detailed simulation methods are exactly as described for the two-stage simulations of Erwin and Miller (1998). For the present paper, the only methodological point needing comment is the concept of a "timestep". Equation 1 is changed by converting $\frac{d}{dt}S^{\mathcal{EC}}(\vec{x},\vec{\alpha},t)$ to $\left[S^{\mathcal{EC}}(\vec{x},\vec{\alpha},t+\Delta t) - S^{\mathcal{EC}}(\vec{x},\vec{\alpha},t)\right]/\Delta t$. We set $\Delta t = 1$, so the learning rate is controlled by the parameter η. A timestep represents one iteration of this equation, that is, updating $S^{\mathcal{EC}}(\vec{x},\vec{\alpha},t)$ to $S^{\mathcal{EC}}(\vec{x},\vec{\alpha},t+1)$. All simulations used $\eta = 0.008$ for the first stage (developing the initial conditions), and $\eta = 0.001$ for the second stage (deprivation and reverse suture). The use of a smaller η simply slows development without affecting its trajectory, and is done to allow stopping the simulation at fairly precise values of percentage of deprivation.

Functions Used

We take all the functions to depend only on distance: $C^{\mathcal{EC},\mathcal{E}'\mathcal{C}'}(\vec{\alpha},\vec{\beta}) = C^{\mathcal{EC},\mathcal{E}'\mathcal{C}'}(|\vec{\alpha}-\vec{\beta}|)$, $A(\vec{x},\vec{\alpha}) = A(|\vec{x}-\vec{\alpha}|)$, $I(\vec{x},\vec{y}) = I(|\vec{x}-\vec{y}|)$.

We assume, for simplicity, that the activity patterns in LGN of the ON and OFF populations are statistically indistinguishable, although in reality, there are differences between ON and OFF spontaneous activity patterns (in retina: Mastronarde, 1983a,b; Wong and Oakley, 1996). Then, the functions $C^{\mathcal{EC},\mathcal{E}'\mathcal{C}'}$ depend only on whether $\mathcal{C}$ and $\mathcal{C}'$ are the same or opposite center types ($S_{\mathcal{C}}$ or $O_{\mathcal{C}}$). Thus, there are only six distinct correlation functions: three describing correlations between two inputs of the same center type (within the left eye, $C^{L_{\mathcal{E}}S_{\mathcal{C}}}$; within the right eye, $C^{R_{\mathcal{E}}S_{\mathcal{C}}}$; and between eyes, $C^{O_{\mathcal{E}}S_{\mathcal{C}}}$, where $O_{\mathcal{E}}$ stands for "opposite eyes"), and similarly, three describing correlations between inputs of opposite center type ($C^{L_{\mathcal{E}}O_{\mathcal{C}}}$, $C^{R_{\mathcal{E}}O_{\mathcal{C}}}$, and $C^{O_{\mathcal{E}}O_{\mathcal{C}}}$).

To establish the initial condition for deprivation, we begin from a random initial condition (each synaptic weight $S^{\mathcal{EC}}(\vec{x},\vec{\alpha})$ chosen randomly from a distribution uniform between $0.8A(\vec{x},\vec{\alpha})$ and $1.2A(\vec{x},\vec{\alpha})$) and carry out development exactly as in the first stage of two-stage development in Erwin and Miller (1998), using the same correlation functions used there. These correlation functions were designed to meet the basic requirements for development of ocularly matched orientation selectivity without development of ocular dominance. To develop orientation-selective simple-cell receptive fields, a given LGN cell should be best correlated with others of its own center type at smaller retinotopic separations, but be best correlated with others of the opposite center type at larger separations (Miller, 1994). The simplest way to cause matching of orientations between the two eyes is to make the between-eye correlations identical to the within-eye correlations. Thus, the correlation functions used are $C^{L_\mathcal{E} S_c} = C^{R_\mathcal{E} S_c} = C^{O_\mathcal{E} S_c} = M/4$, $C^{L_\mathcal{E} O_c} = C^{R_\mathcal{E} O_c} = C^{O_\mathcal{E} O_c} = -M/4$ (corresponding to $C^{\text{ORI+}} = M$, $C^{\text{OD}} = C^{\text{SUM}} = C^{\text{ORI}-} = 0$, in terms of the composite correlation functions described in Erwin and Miller 1998), where M is an oscillating "Mexican hat" function, defined in terms of Gaussian functions G_γ:

$$G_\gamma(\vec{\alpha} - \vec{\beta}) = (1/\gamma^2) \exp[-|\vec{\alpha} - \vec{\beta}|^2/((0.24\gamma)(6.5))^2] \tag{5}$$

$$M(\vec{\alpha} - \vec{\beta}) = G_1(\vec{\alpha} - \vec{\beta}) - G_3(\vec{\alpha} - \vec{\beta}). \tag{6}$$

The functions M and G_3 are illustrated in Fig. 2a,b. The only free parameter in development of the initial condition is the number of timesteps, t_1, of this initial development.

Place Fig. 2 about here

Beginning from this initial condition, we simulate deprivation followed by reverse suture. We assume that, in the absence of deprivation, development would have proceeded as in the second stage of development in Erwin and Miller (1998). Correlations in that stage were modified to cause development of ocular dominance. This required an overall correlation within each eye that was independent of center type, which was achieved by adding a spatially broad, non-oscillating second component, modeled by the function G_3, to both same-center-type and opposite-center-type correlations. We assume that monocular deprivation leaves correlations within the open eye unchanged, and so make these correlations identical to those existing within each eye in the second stage of development in Erwin and Miller (1998). Letting $N_\mathcal{E}$ stand for the non-deprived, open eye, the open-eye correlation functions in the second stage are $C^{N_\mathcal{E} S_c} = \frac{1}{4}(M + dG_3)$ and $C^{N_\mathcal{E} O_c} = \frac{1}{4}(-M + dG_3)$, Fig. 2c,d, (derived from $C^{\text{ORI+}} = M$, $C^{\text{OD}} = dG_3$, $C^{\text{ORI}-} = C^{\text{SUM}} = 0$). Increases of the constant d represent increased strength of the drive toward development of ocular dominance relative to the drive toward development of orientation. Two examples of these correlation functions are illustrated in Fig. 2c–d.

Correlations within a deprived eye are simulated in two possible forms (Fig. 2e–f). To simulate deprivation with TTX, the correlations are set to zero. To simulate deprivation through eyelid suture, we used broad Gaussian functions, with opposite signs for same center-type vs. opposite center-type, to represent the correlations that would be expected to occur due to light transmission through the closed eyelids. Letting $D_\mathcal{E}$ stand for the deprived eye, these are set to $C^{D\varepsilon Sc} = \frac{1}{4}(G_3)$ and $C^{D\varepsilon Oc} = -\frac{1}{8}(G_3)$. Between-eye correlations are set to zero during deprivation and reverse suture.

We continue to use the intracortical interaction function $I(\vec{x}, \vec{y})$ and the arbor function $A(\vec{x}, \vec{y})$ used in Erwin and Miller (1998), and to vary only the correlation functions, as in that paper. The influence of these functions on development was described in Miller (1994); changes in them will have little impact on the interactions between ocular dominance and orientation studied here (as discussed in Erwin & Miller, 1998).

Methods of carrying out deprivation and reverse suture

We assess the ocular dominance m of a given cortical cell at $\vec{x}$ as the difference between the left-eye and right-eye synaptic strength received by the cell, divided by their sum:

$$m(\vec{x}) = \frac{\sum_{\vec{\alpha}} S^{LN}(\vec{x}, \vec{\alpha}) + S^{LF}(\vec{x}, \vec{\alpha}) - S^{RN}(\vec{x}, \vec{\alpha}) - S^{RF}(\vec{x}, \vec{\alpha})}{\sum_{\vec{\alpha}} S^{LN}(\vec{x}, \vec{\alpha}) + S^{LF}(\vec{x}, \vec{\alpha}) + S^{RN}(\vec{x}, \vec{\alpha}) + S^{RF}(\vec{x}, \vec{\alpha})}.$$

The average ocular dominance $\langle m \rangle$ is the average of $m(\vec{x})$ over all $\vec{x}$, *i.e.* over all cortical cells. We carry out deprivation until $\langle m \rangle$ is equal to some target value T (*e.g.* 60%), and then reverse the suture and continue until $\langle m \rangle = -T$. Results at $\langle m \rangle = T$ (after initial deprivation) are compared to those at $\langle m \rangle = -T$ (after reverse suture), and these comparisons are shown as a function of T, which represents the strength of the deprivation.

In some cases, we model deprivation as a random deletion of synapses from the deprived eye, rather than as a gradual loss of synaptic strength under activity patterns simulating deprivation. To implement this, for a given target level T, we first ran an ordinary forward deprivation simulation until $\langle m \rangle = T$. The strengthened open-eye synaptic strengths were kept. However, rather than use the closed-eye synaptic strengths that resulted from the deprivation, the closed-eye synaptic strengths were instead set back to their initial, pre-deprivation values and then, for each cortical cell, closed-eye synapses were deleted (set to strength zero) at random until the cell's total closed-eye synaptic strength was less than or equal to the value it had reached under the deprivation. We then reversed the suture until $\langle m \rangle = -T$.

Assessment of Correlation Between Orientation Maps

To determine the similarity of any two orientation maps, A and B, we first compute single-orientation response maps, $A(\vec{x}, \theta)$ and $B(\vec{x}, \theta)$, as a function of cortical position $\vec{x}$ at a set of discrete orientations θ. Correlation coefficients (Pearson's r, Press et al., 1992) are computed between the two single-orientation maps, giving a measure $r(\theta)$, which is then averaged over θ to give a single measure of similarity between the maps. This is the method used in the optical imaging experiments of Godecke and Bonhoeffer (1996) as well as in Erwin and Miller (1998). We define the responses, $A(\vec{x}, \theta)$ and $B(\vec{x}, \theta)$, as the maximum LGN input to cells at $\vec{x}$ due to any grating (of any spatial phase or frequency) with preferred orientation within $\pm 5^\circ$ of θ, using 18 orientations at 10° intervals.

Results

In previous work, we showed how ocularly matched orientation maps and ocular dominance segregation can codevelop through competition between ON- and OFF-center geniculocortical inputs serving left and right eyes (Erwin & Miller, 1998). Here we use the framework of that study to address the effects of deprivation and reverse suture.

Initial Conditions For Studying Deprivation

In our previous study (Erwin & Miller, 1998), we considered two developmental scenarios. In a "one-stage" scenario, ocularly-matched orientation maps and ocular dominance codevelop based on LGN activity patterns with a fixed correlation structure. In a "two-stage" scenario, ocularly matched orientation maps begin to develop under one correlation structure, and subsequently ocular dominance maps develop (and orientation maps mature) under an altered correlation structure. With appropriate LGN activity correlation structures, either scenario can account for many basic features of visual cortical development. In this paper, we will use the two-stage scenario. Results using the one-stage scenario are entirely similar.

Thus, we assume that deprivation is initiated after the first stage of development, at which point ocularly matched orientation maps have partially developed but ocular dominance maps have not begun to form. This assumption represents two statements about the biology. First, it represents the idea that a weak, ocularly matched orientation map has developed in the two eyes before deprivation affects development. As discussed in the Introduction, this is well supported by experimental results (Crair et al., 1998; Fregnac & Imbert, 1984; Movshon & Van Sluyters, 1981; Shatz & Stryker, 1978). Second, it represents the idea that ocular dominance development has not begun before deprivation affects development. This is probably an oversimplification (*e.g.*, see Crair et al., 1998; Crowley & Katz, 2000). However, previous theoretical studies (Miller et al., 1989) demonstrated that initiating deprivation later and later in ocular dominance development simply lessens the deprivation effects. Thus, our assumption simply means that the strongest possible deprivation effects can be attained. This provides the strongest possible challenge to the ability to restore a map after reverse suture, and thus is a conservative assumption.

In this paper, the first stage of development is used only as a means of generating the initial condition — ocularly matched orientation maps without ocular dominance — for studying the effects of deprivation. Thus, for present purposes the only important parameter describing the first stage is its duration: a longer first stage corresponds to increased maturity of the orientation map, and increased binocular correlation of orientation maps, before the onset of deprivation. We refer to the length of the first stage as t_1. We initially consider the case $t_1 = 26$ (in arbitrary units of simulation "timesteps", see Methods), a relatively short time that allows only weak development of orientation maps in the first stage. We will subsequently show the effects of increasing t_1.

Place Fig. 3 about here

A typical initial condition for deprivation — the end of the first stage of development — for $t_1 = 26$ is shown in the top rows of Fig. 3 (orientation maps) and Fig. 4 (receptive fields of the 8×8 cells with locations indicated by the white squares in Fig. 3). Receptive fields and orientation selectivity are only weakly developed. The two eyes' orientation maps are only imperfectly correlated, with a correlation coefficient of 0.71. This binocular matching of the maps was induced by appropriate between-eye activity correlations during the first stage of development. The maps would become almost perfectly correlated if the first stage were continued longer (see Fig. 5).

Place Fig. 4 about here

Monocular Deprivation

Beginning with the given initial condition, the second stage of development uses LGN activity correlations that model deprivation. There are no longer any correlations between the activities of the two eyes. The only activity correlations are among inputs within a single eye. The correlation patterns within the open, normal eye differ from those within the deprived eye, in a manner that models deprivation effects. The LGN correlations within the open eye contain the basic structures we have shown are needed to ensure development of orientation and ocular dominance (see Methods). The strength of the drive toward development of ocular dominance, relative to that toward development of orientation selectivity, is parameterized by a constant d. We initially consider the case $d = 2$.

We begin by considering a case in which all closed-eye activity correlations are described by a a small-magnitude, spatially broad function, positive for same-center-type inputs and negative for opposite-center-type inputs, representing the effects of diffuse light penetrating closed eyelids, Fig. 2f. We will subsequently consider an alternative in which closed-eye correlations are set to zero, representing the effect of TTX infusion in that eye, Fig. 2e. The stronger activity correlations in the open eye, along with the competitive mechanisms, cause the strength of the open eye's synapses to increase and the strength of the closed eye's synapses to decrease, yielding the familiar "monocular deprivation shift" in ocular dominance in favor of the open eye, Figs. 3-4 (row B).

We allow deprivation to proceed until 60% of deprived-eye (right-eye) synaptic strength has been eliminated. At this point, the right eye responds only weakly to stimulation (indicated by low brightness in row B of Fig. 3 and in left side of Fig. 4). Yet responses evoked by this deprived eye still show detectable preferred orientations at many locations, as is also observed experimentally (Antonini et al., 1998; Crair et al., 1997).

Since the left eye was presented with normal within-eye correlation functions, its synaptic strengths have grown stronger than in the earlier map, and it shows robust orientation-tuned responses arranged in a mature map (Fig. 3). However, its receptive fields are still only very weakly segregated into ON and OFF subregions (Fig. 4). With more time to develop, they would completely segregate; such complete segregation is seen at this point if deprivation is begun from a more developed initial condition (larger t_1).

Reverse Suture

Beginning from the condition shown in Figs. 3-4, row B, we now reverse the deprivation by interchanging the right- and left-eye correlation functions, restoring normal activity to the previously deprived eye and imposing the activity pattern modeling deprivation in the previously normal eye. Development continues until the newly deprived eye's synaptic strength is reduced to the same level as had been achieved in the initially deprived eye. The condition after reverse deprivation is shown in Figs. 3-4, row C. The newly opened eye regains a strong response, with an orientation map very similar to that which existed in the previously opened eye (row B). Although most synaptic strength was eliminated in the originally deprived eye, the synaptic strengths that remained retained enough information from the original orientation map of row A to "seed" the process and ensure development of a very similar map.

The correlation coefficient between the map emerging in the newly opened eye after reverse deprivation (bottom row, right eye), and that existing in the initially open eye after the initial monocular deprivation (row B, left eye), is 0.795. This falls within the experimentally observed range of 0.75-0.9 (Gödecke & Bonhoeffer, 1996). Surprisingly, this correlation coefficient is *greater* than that (0.71) which existed between the two eyes' maps before the onset of deprivation (row A), even though there were no between-eye correlations during deprivation or reverse suture.

The basis for this result was first shown in Erwin and Miller (1998), Fig. 12. There we showed that, beginning from the initial condition of Figs. 3-4, top row, subsequent *independent* development of the orientation maps in the two eyes led each map to converge to a common final state; the correlation between the two eye's maps steadily increased to near 1. That is, the initial maps, although only weakly developed, were sufficiently developed to specify the subsequent course and final fate of orientation map development; and each eyes' map specified the same fate despite their still-imperfect correlation with one another. We may say that the orientation map's fate was dynamically committed. The present result shows that this dynamical fate commitment is not greatly perturbed even by the loss of 60%

of deprived-eye synaptic strength through monocular deprivation.

Parameter Dependence

The similarity of the orientation maps observed after initial deprivation and after reverse suture is quite robust. The correlation between the maps remains within the experimentally observed range (.75–.9) across multiple simulations using a variety of random initial conditions and parameters, varying extents of initial development before deprivation (corresponding to variation in t_1), and varying extents of deprivation, Fig. 5A. We consider two models of deprived-eye activity, either an absence of activity (Fig. 5, "TTX"), or unpatterned activity representing light transmission through a closed eyelid as in Fig. 3 (Fig. 5, "Non-TTX"). We also considered various values of the parameter d that controls the strength of the broad, ocular-dominance-favoring component in the activity correlations of the open eye. For all parameters studied, the extent of the degradation of deprived-eye synaptic connections would need to be great — a reduction of 60-90% — before the orientation map that re-develops in the initially-deprived eye would fall outside the experimentally observed range of correlation with the map in the initially open eye. *Place Fig. 5 about here*

One may worry that the model deprivation may simply scale down synaptic strengths without greatly disrupting their pattern, and that this might not be an accurate model of real deprivation. We control for this in two ways. First, we examine the same data in terms of the percentage of deprived-eye synapses that were deleted (driven to zero strength) by the deprivation, Fig. 5B. When deprivation was begun at the latest time studied ($t_1 = 66$), 75-85% of deprived-eye synapses were lost to deprivation without loss of "memory" of the orientation map. Deprivations begun at earlier times, however, led to fewer synapses reaching the upper and lower limits and hence to elimination of fewer synapses. *Place Fig. 6 about here*

Second, we implemented deprivation as a random pruning of deprived-eye synapses rather than as a gradual loss of synaptic strength. A typical example is shown in Figs 6-7. The initial condition (top rows) is somewhat more developed than in the previous example ($t_1 = 46$): receptive fields show good ON/OFF segregation, and the two eyes' maps are almost perfectly correlated. Deprivation by random synaptic pruning was carried out until 70% of deprived-eye synaptic strength was lost. This devastated the deprived-eye receptive fields, leaving only *Place Fig. 7 about here* slivers of innervation (Fig. 7, middle row). Yet after reverse deprivation, a map much like that of the originally opened eye is restored (Fig. 6, bottom row, right eye, compare middle row, left eye). The correlation between these two maps is 77%. Results vs. parameters for deprivation by random synaptic pruning (Fig. 8) show that, if the initial condition is sufficiently developed that receptive fields show reasonable ON/OFF segregation and maps are well correlated – $t_1 = 46$ (Figs 6-7, top row) or $t_1 = 66$ – then 60-80% loss of strength through random synaptic deletion does not erase the memory of the map. However, when the initial condition is only weakly developed ($t_1 = 26$, Figs. 3-4, top row), with little ON/OFF segregation in receptive fields and only 71% binocular correlation in orientation maps, even a small amount of random synaptic deletion largely destroys the memory of the map.

Place Fig. 8 about here

These results can be understood as follows. When there is little ON/OFF segregation in receptive fields, random deletion of synapses will create random regions in which ON or OFF inputs dominate the receptive field. Subsequent development will carve ON/OFF subregions that tend to correctly overlap these random regions, and hence to choose an orientation very different than that toward which the poorly segregated receptive field had been biased. In contrast, if the poorly segregated receptive field is subject to a more continuous form of deprivation, ON and OFF inputs will tend to be equally affected and the initial biases of the receptive field may remain roughly intact. In addition, because nearby cells influence one another to have similar preferred orientations, it is enough if on average the biases of small groups of cells remain intact. Once a receptive field has reasonable ON/OFF segregation, random synaptic deletion will leave a sparse patchwork of ON and OFF inputs in locations compatible with the pre-deprivation arrangement of subregions and thus with the pre-deprivation preferred orientation. Even though this patchwork shows little sign of the cell's preferred orientation (Fig. 7, middle row), it is enough – again, averaged over local groups of cells – to seed development back to a similar arrangement of ON and OFF subregions as existed prior to the synaptic deletion, and thus back to a similar preferred orientation. ON subregions and OFF subregions are well segregated physiologically in cat V1 simple cells well before the onset of the critical period (Albus and Wolf, 1984; Braastad and Heggelund, 1985; Fregnac and Imbert, 1984; Hubel and Wiesel, 1963; see also discussion in DeAngelis et al., 1993). Thus, the model regime in which maps are resilient even to random synaptic deletion is likely to apply to cat development.

Discussion

The paradigm of monocular deprivation and reverse suture, along with the evidence that cat orientation selectivity is determined by the organization of geniculocortical afferents (*e.g.*, Ferster et al., 1996; Ferster & Miller, 2000; Reid & Alonso, 1995), posed a prominent challenge to the hypothesis of activity-instructed, correlation-based cortical map development. Here, that challenge is answered by the combination of three findings. First, experimentally, the development of binocularly matched maps has begun well before the onset of deprivation effects, as discussed in the Introduction. Modelling studies have demonstrated how this matching can be achieved by activity-instructed development of geniculocortical connections (Erwin & Miller, 1998). Second, once early development of matched maps has progressed sufficiently, modelling studies (Erwin & Miller, 1998) indicate that the fates of the maps are committed dynamically. After this point, even if the two eyes' maps develop independently, they will converge upon the same final outcome under activity-instructed development of geniculocortical connections. Third, we have shown here that this dynamically committed fate survives even the massive synaptic depletion of monocular deprivation, followed by reverse suture. As a result, the maps of the two open eyes, one observed after monocular deprivation and the other after reverse suture, are well matched, despite losses of 60-80% of one eye's geniculocortical synaptic strength during the initial deprivation, and despite a complete absence of binocular correlation in input activity patterns during the period of deprivation and reverse suture. If ON and OFF subregions are reasonably segregated in receptive fields before the onset of deprivation effects, as appears to be the case (Albus & Wolf, 1984; Braastad & Heggelund, 1985; Fregnac & Imbert, 1984; Hubel & Wiesel, 1963), then these maps are well matched even when deprivation is modelled as random pruning of synapses in the deprived eye.

The surprise in the present results is quantitative rather than qualitative. It is not surprising that a sufficient residue of a pre-existing map will seed a very similar map. What seems surprising is that, even after the massive disruptions of the pre-existing receptive fields studied here (*e.g.*, Fig. 7), the remaining residue is sufficient. To connect this to the experimental studies, it must be the case that the disruptions that we study are comparable to (or greater than) the disruption induced by monocular deprivation. Two lines of evidence support this. First, even after long monocular deprivation, a weak but otherwise relatively normal orientation map can still be observed in response to stimulation of the deprived eye (Antonini et al., 1998; Crair et al., 1997). Second, although it is difficult to assess the extent of synaptic degradation in physiological experiments, anatomical results appear consistent with our model: monocular deprivation from birth to P39 in kittens results in no more than a 60% reduction in the total length of LGN arbors relative to normal kittens of the same age (Antonini et al., 1998; Antonini & Stryker, 1993, 1996), and synaptic density along the arborization of deprived-eye axons is normal (Silver & Stryker, 1999). This is suggestive that even prolonged deprivation does not remove more than 60% of deprived-eye synaptic strength, a figure well within the range studied here.

Alternative Mechanisms of Ocular Matching of Orientation Maps

Several mechanisms not considered here might also contribute to ocular matching of orientation maps.

We have assumed that there are no interocular activity correlations during deprivation. However, interocular LGN correlations that do not depend on vision exist in early development (Weliky & Katz, 1999), and these might persist during deprivation, albeit diluted by the monocular correlations induced by vision in the open eye. Interocular correlations would presumably only aid in the matching of the two eyes' maps, and thus allow even greater loss of deprived-eye synaptic strength to occur while still yielding matched maps after reverse suture.

Our model uses a very impoverished picture of intracortical connections, assuming these depend only on horizontal separation, are isotropic, and are unchanging during development. This is sufficient to study development of receptive field structure in geniculocortical connections and to model basic aspects of map structure like local continuity of preferred orientation, but better models of cortical circuitry are needed to address more detailed aspects of map structure (discussed in Miller, 1994). Long-range horizontal intracortical connections codevelop along with the geniculocortical connections (Durack & Katz, 1996; Ruthazer & Stryker, 1996), as most likely do short-range connections, and at least the longer-range connections develop orientation-specific anisotropies (Bosking et al., 1997; Schmidt et al., 1997). These anisotropies could contribute to binocular map matching: for example, if connections to or from a given cortical point extend preferentially in the retinotopically vertical direction, this might be sufficient to bias cortical cells at that point to develop a vertical preferred orientation under activity-instructed rules, and this would be a common cortical influence on maps of both eyes. Indeed, modelers have shown that either short-range (Bartsch & van Hemmen, 2001) or long-range (Shouval et al., 2000) connections with strong such biases could suffice to largely specify subsequent development of an orientation map. However, long-range connections show only weak clustering before eye-opening (Durack & Katz, 1996; Ruthazer & Stryker, 1996) and so are likely to show only at most weak biases at the time that orientation maps initially develop; the case for short-range connections is unknown. It will be of interest to theoretically explore whether weak biases in intracortical connections could also be sufficient to specify map structure.

The boundary conditions of cat cortical area 18 have also been proposed to provide an external cue specifying orientation map structure. Wolf et al. (1996) showed that, for distances from an areal boundary on the order of the orientation periodicity, activity-instructed development could cause well-correlated orientation maps to develop from different (but statistically identical) patterns of input activity, starting from identical sets of initial weights. Because area 18 is long and thin, all of it is within a few millimeters from a boundary and hence all of its orientation map could be so specified. Whether this result is robust to non-identical initial distributions of the left eye's and right eye's weights is unclear; otherwise it is intriguing.

If boundary effects were the only cue linking the two eyes' maps, then orientation maps developed in the absence of binocularly common visual experience should not be binocularly matched in area 17 at distances more than a few millimeters from the area 17/18 boundary. Our model predicts instead that map matching should occur throughout area 17 as well as area 18. At present, mapping data comes only from near the area 17/18 border or from area 18 (Crair et al., 1998; Gödecke & Bonhoeffer, 1996) and not from further inside area 17.

Thus, the definitive test remains to be done. On a cell-by-cell basis, significant inter-eye discrepancies in preferred orientation were observed in area 17 after reverse suture (Movshon, 1976) (no such measurements have been made in area 18). This has been interpreted (Wolf et al., 1996) to suggest that area 17 orientation maps are not restored after reverse suture. However, comparison of the two eyes after reverse suture, as in Movshon (1976), should be contrasted with comparison between the open eye after initial deprivation and the newly opened eye after reverse suture, as in Godecke and Bonhoeffer (1996). In our simulations, the latter yields a somewhat narrower distribution of orientation discrepancies on a cell-by-cell basis than the former (unpublished results).

Our modeling shows that none of the above factors are necessary to explain the reverse suture experiments; the initial structure of the geniculocortical connections existing before the onset of deprivation effects is sufficient. Of course, these factors may nonetheless contribute to map matching.

Experimental Predictions and Implications

The present work provides evidence for an overall framework — activity-instructed, correlation-based self-organization of orientation maps in cat layer 4 via plasticity of geniculocortical connections. The major experimental impact of the present work is to show that existing experimental results on reverse suture that had been thought to argue against this framework actually are expected from this framework.

This framework of activity-instructed development makes many testable predictions, as have been described (Erwin & Miller, 1998, 1999; Miller, 1994). The central predictions are that the correlations in spontaneous LGN activity during the time that orientation develops should have certain simple forms. One key prediction is that, among the inputs serving a single eye, a competition between ON-center and OFF-center inputs, involving a certain intraocular correlation structure among these inputs, drives the development of simple cells and orientation selectivity. A test of this prediction was recently made in ferrets by binocularly eliminating ON-center retinal activity, leaving OFF-center activity intact; the result, consistent with the model, was that the development of orientation selectivity was prevented (Chapman & Gödecke, 2000). A second key prediction is that binocular matching of preferred orientations arises from a particular structure of interocular activity correlations. The presence of strong interocular correlations has been demonstrated in developing ferret LGN in the absence of vision (Weliky & Katz, 1999), but whether these had the structure predicted could not be determined. These issues would actually best be studied in cat LGN, since in cat, but not ferret (Chapman & Stryker, 1993), orientation selectivity is well developed in the geniculate-recipient layer 4.

Are the required correlation structures plausible? We have previously argued (Miller, 1994) that the required intraocular correlation structure between ON- and OFF-center inputs are a plausible attribute of spontaneous activity, as they would arise if such activity is driven by the filtering of photoreceptor noise (Mastronarde, 1989) by LGN receptive fields. It is less clear what correlation structure would arise from natural vision after eye opening. However, two lines of evidence suggest that visually-driven LGN activities may also show the correlations required to segregate ON and OFF subregions within simple cell receptive fields. First, a model of Hebb-like learning driven by natural scenes filtered by center-surround receptive fields was shown to produce such segregation (Lee et al., 2000). Second, experiments show that lid suture, which passes only very low spatial frequencies of light stimulation and so would be expected to disrupt the required correlation structure (by causing spatially widespread positive correlations within each center type), disrupts the orientation selectivity that developed before eye opening; while in contrast, dark-rearing (which should preserve the spontaneous correlation structure) leaves intact, and natural vision increases, the degree of orientation selectivity relative to that existing at eye opening (White et al., 2001). It is less clear what mechanisms could yield the structure of interocular correlations in spontaneous activity required to initially binocularly match the maps (see discussion in Erwin & Miller, 1998), but ultimately the proof will be in experimental measurements.

The present work also adds some new predictions. Our previous work (Erwin & Miller, 1998) predicts that all of area 17, as well as area 18, should develop binocularly correlated orientation maps before the onset of deprivation. The current work adds the predictions that orientation maps measured after monocular deprivation and reverse suture should be matched where, and only where, such early binocularly correlated maps exist. In particular, such matching should occur throughout area 17 provided that early maps there are binocularly correlated.

In conclusion, we believe our results demonstrate the resilience of orientation maps to massive degradation by monocular deprivation, and by implication the resilience of the hypothesis that orientation selectivity develops by activity-instructed competition among geniculocortical afferents.

Acknowledgements: We gratefully acknowledge useful conversations with and/or helpful comments on early versions of the manuscript from Steve Lisberger, Michael Crair, Ed Ruthazer, and Michael Stryker; and we thank the latter three and Deda Gillespie for sharing their experimental results with us at preliminary stages. We gratefully acknowledge support by the NIH (grants NS07067 and EY11001).

References

Albus, K. & Wolf, W. (1984). Early post-natal development of neuronal function in the kitten's visual cortex: A laminar analysis. *J. Physiol.*, 348, 153–185.

Antonini, A., Gillespie, D. C., Crair, M. C., & Stryker, M. P. (1998). Morphology of single geniculocortical afferents and functional recovery of the visual cortex after reverse monocular deprivation in the kitten. *J. Neurosci.*, 18, 9896–9909.

Antonini, A. & Stryker, M. P. (1993). Rapid remodeling of axonal arbors in the visual cortex. *Science*, 260, 1819–1821.

Antonini, A. & Stryker, M. P. (1996). Plasticity of geniculocortical afferents following brief or prolonged monocular occlusion in the cat. *J. Comp. Neurol.*, 369, 64–82.

Bartsch, A. P. & van Hemmen, J. L. (2001). Combined Hebbian development of geniculocortical and lateral connectivity in a model of primary visual cortex. *Biol. Cybern.*, 84, 41–55.

Bienenstock, E. L., Cooper, L. N., & Munro, P. W. (1982). Theory for the development of neuron selectivity: Orientation specificity and binocular interaction in visual cortex. *J. Neurosci.*, 2, 32–48.

Bosking, W. H., Zhang, Y., Schofield, B., & Fitzpatrick, D. (1997). Orientation selectivity and the arrangement of horizontal connections in tree shrew striate cortex. *J. Neurosci.*, 17, 2112–2127.

Braastad, B. O. & Heggelund, P. (1985). Development of spatial receptive-field organization and orientation selectivity in kitten striate cortex. *J. Neurophysiol.*, 53, 1158–1178.

Chapman, B. & Gödecke, I. (2000). Cortical cell orientation selectivity fails to develop in the absence of on-center retinal ganglion cell activity. *J. Neurosci.*, 20, 1922–1930.

Chapman, B. & Stryker, M. P. (1993). Development of orientation selectivity in ferret visual cortex and effects of deprivation. *J. Neurosci.*, 13, 5251–5262.

Chapman, B., Stryker, M. P., & Bonhoeffer, T. (1996). Development of orientation preference maps in ferret primary visual cortex. *J. Neurosci.*, 16, 6443–6453.

Crair, M. C., Gillespie, D. C., & Stryker, M. P. (1998). The role of visual experience in the development of columns in cat visual cortex. *Science*, 279, 566–570.

Crair, M. C., Ruthazer, E. S., Gillespie, D. C., & Stryker, M. P. (1997). Relationship between the ocular dominance and orientation maps in visual cortex of monocularly deprived kittens. *Neuron*, 19, 307–318.

Crowley, J. C. & Katz, L. C. (1999). Development of ocular dominance columns in the absence of retinal input. *Nature Neurosci.*, 2, 1125–1130.

Crowley, J. C. & Katz, L. C. (2000). Early development of ocular dominance columns. *Science*, 290, 1321–1324.

Davis, G. W. & Goodman, C. S. (1998). Synapse-specific control of synaptic efficacy at the terminals of a single neuron. *Nature*, 392, 82–86.

DeAngelis, G. C., Ohzawa, I., & Freeman, R. D. (1993). Spatiotemporal organization of simple-cell receptive fields in the cat's striate cortex. I. General characteristics and postnatal development. *J. Neurophysiol.*, 69, 1091–1117.

Durack, J. C. & Katz, L. C. (1996). Development of horizontal projections in layer 2/3 of ferret visual cortex. *Cerebral Cortex*, 6, 178–183.

Ernst, U. A., Pawelzik, K. R., Sahar-Pikielny, C., & Tsodyks, M. V. (2001). Intracortical origin of visual maps. *Nature Neurosci.*, 4, 431–436.

Erwin, E. & Miller, K. D. (1996). A correlation-based model explains the monocular deprivation effects on orientation and ocularity maps and orientation recovery after reverse deprivation. *Soc. Neurosci. Abstr.*, 22, 1727.

Erwin, E. & Miller, K. D. (1998). Correlation-based development of ocularly-matched orientation maps and ocular dominance maps: Determination of required input activity structures. *J. Neurosci.*, 18, 9870–9895.

Erwin, E. & Miller, K. D. (1999). The subregion correspondence model of binocular simple cells. *J. Neurosci.*, 19, 7212–7229.

Ferster, D., Chung, S., & Wheat, H. (1996). Orientation selectivity of thalamic input to simple cells of cat visual cortex. *Nature*, 380, 249–252.

Ferster, D. & Miller, K. D. (2000). Neural mechanisms of orientation selectivity in the visual cortex. *Ann. Rev. Neurosci.*, 23, 441–471.

Fregnac, Y. & Imbert, M. (1984). Development of neuronal selectivity in the primary visual cortex of the cat. *Physiol. Rev.*, 64, 325–434.

Gödecke, I. & Bonhoeffer, T. (1996). Development of identical orientation maps for two eyes without common visual experience. *Nature*, 379, 251–254.

Guillery, R. W. (1972). Binocular competition in the control of geniculate cell growth. *J. Comp. Neurol.*, 144, 117–130.

Hubel, D. H. & Wiesel, T. N. (1963). Receptive fields of cells in striate cortex of very young, visually inexperienced kittens. *J. Neurophysiol.*, 26, 994–1002.

Katz, L. C. & Shatz, C. J. (1996). Synaptic activity and the construction of cortical circuits. *Science*, 274, 1133–1138.

Lee, A. B., Blais, B., Shouval, H. Z., & Cooper, L. N. (2000). Statistics of lateral geniculate nucleus (LGN) activity determine the segregation of ON/OFF subfields for simple cells in visual cortex. *Proc. Natl. Acad. Sci. USA*, 97, 12875–12879.

Mastronarde, D. N. (1983a). Correlated firing of cat retinal ganglion cells. I. Spontaneously active inputs to X and Y cells. *J. Neurophysiol.*, 49, 303–324.

Mastronarde, D. N. (1983b). Correlated firing of cat retinal ganglion cells. II. Responses of X- and Y-cells to single quantal events. *J. Neurophysiol.*, 49, 325–349.

Mastronarde, D. N. (1989). Correlated firing of retinal ganglion cells. *Trends Neurosci.*, 12, 75–80.

Miller, K. D. (1990). Derivation of linear Hebbian equations from a nonlinear Hebbian model of synaptic plasticity. *Neural Comput.*, 2, 321–333.

Miller, K. D. (1994). A model for the development of simple cell receptive fields and the ordered arrangement of orientation columns through activity-dependent competition between ON- and OFF-center inputs. *J. Neurosci.*, 14, 409–441.

Miller, K. D. (1996a). Receptive fields and maps in the visual cortex: Models of ocular dominance and orientation columns. In Domany, E., van Hemmen, J. L., & Schulten, K., editors, *Models of Neural Networks III*, pages 55–78. Springer-Verlag, New York. Available as ftp://ftp.keck.ucsf.edu/pub/ken/miller95.ps.

Miller, K. D. (1996b). Synaptic economics: Competition and cooperation in synaptic plasticity. *Neuron*, 17, 371–374.

Miller, K. D. (1998). Equivalence of a sprouting–and–retraction model and correlation–based plasticity models of neural development. *Neural Comput.*, 10, 529–547.

Miller, K. D., Keller, J. B., & Stryker, M. P. (1989). Ocular dominance column development: Analysis and simulation. *Science*, 245, 605–615.

Miller, K. D. & MacKay, D. J. C. (1994). The role of constraints in Hebbian learning. *Neural Comput.*, 6, 100–126.

Movshon, J. A. (1976). Reversal of the physiological effects of monocular deprivation in the kitten's visual cortex. *J. Physiol.*, 261, 125–174.

Movshon, J. A. & Van Sluyters, R. C. (1981). Visual neural development. *Ann. Rev. Psychol.*, 32, 477–522.

Press, W. H., Teukolsky, S. A., Vetterling, W. T., & Flannery, B. P. (1992). *Numerical Recipes in C.* Cambridge University Press, Cambridge, second edition.

Reid, R. C. & Alonso, J. M. (1995). Specificity of monosynaptic connections from thalamus to visual cortex. *Nature*, 378, 281–284.

Ruthazer, E. S. & Stryker, M. P. (1996). The role of activity in the development of long-range horizontal connections in area 17 of the ferret. *J. Neurosci.*, 15, 7253–7269.

Schmidt, K. E., Goebel, R., Löwel, S., & Singer, W. (1997). The perceptual grouping criterion of colinearity is reflected by anisotropies of connections in the primary visual cortex. *Eur. J. Neurosci.*, 9, 1083–1089.

Shatz, C. J. & Stryker, M. P. (1978). Ocular dominance in layer IV of the cat's visual cortex and the effects of monocular deprivation. *J. Physiol.*, 281, 267–283.

Shouval, H. Z., Goldberg, D. H., Jones, J. P., Beckerman, M., & Cooper, L. N. (2000). Structured long-range connections can provide a scaffold for orientation maps. *J. Neurosci.*, 20, 1119–1128.

Silver, M. A. & Stryker, M. P. (1999). Synaptic density in geniculocortical afferents remains constant after monocular deprivation in the cat. *J. Neurosci.*, 19, 10829–10842.

Song, S., Miller, K. D., & Abbott, L. F. (2000). Competitive Hebbian learning through spike-timing-dependent synaptic plasticity. *Nature Neuroscience*, 3, 919–926.

Stryker, M. P. & Harris, W. A. (1986). Binocular impulse blockade prevents the formation of ocular dominance columns in cat visual cortex. *J. Neurosci.*, 6, 2117–2133.

Stryker, M. P. & Strickland, S. L. (1984). Physiological segregation of ocular dominance columns depends on the pattern of afferent electrical activity. *Inv. Opthal. Supp.*, 25, 278.

Turrigiano, G. G., Leslie, K. R., Desai, N. S., Rutherford, L. C., & Nelson, S. B. (1998). Activity-dependent scaling of quantal amplitude in neocortical neurons. *Nature*, 391, 892–896.

Turrigiano, G. G. & Nelson, S. B. (2000). Hebb and homeostasis in neuronal plasticity. *Curr. Opin. Neurobiol.*, 10.

von der Malsburg, C. (1973). Self-organization of orientation selective cells in the striate cortex. *Kybernetik*, 14, 85–100.

Weliky, M. & Katz, L. C. (1997). Disruption of orientation tuning in primary visual cortex by artificially correlated neuronal activity. *Nature*, 386, 680–685.

Weliky, M. & Katz, L. C. (1999). Correlational structure of spontaneous neuronal activity in the developing lateral geniculate nucleus *in vivo*. *Science*, 285, 599–604.

White, L. E., Coppola, D. M., & Fitzpatrick, D. (2001). The contribution of sensory experience to the maturation of orientation selectivity in ferret visual cortex. *Nature*, 411, 1049–1052.

Wiesel, T. N. & Hubel, D. H. (1974). Ordered arrangement of orientation columns in monkeys lacking visual experience. *J. Comp. Neurol.*, 158, 307–318.

Wolf, F., Bauer, H.-U., Pawelzik, K., & Geisel, T. (1996). Organization of the visual cortex. *Nature*, 382, 306.

Wong, R. O. & Oakley, D. M. (1996). Changing patterns of spontaneous bursting activity of On and Off retinal ganglion cells during development. *Neuron*, 16, 1087–1095.

Figure Legends

Figure 1. A schematic diagram of the model showing the meaning of the variables. The synaptic weight, $S^{\mathrm{RN}}(\vec{x}, \vec{\alpha})$, represents the connection strength from the right-eye (R), ON-center (N) LGN cell at position $\vec{\alpha}$ to the cortical cell at position $\vec{x}$. Similarly, $S^{\mathrm{RF}}(\vec{y}, \vec{\beta})$ represents the right-eye (R), OFF-center (F) weight from $\vec{\beta}$ to $\vec{y}$, while $S^{\mathrm{LN}}(\vec{y}, \vec{\beta})$, $S^{\mathrm{LF}}(\vec{y}, \vec{\beta})$ are the corresponding left-eye ON- and OFF-center weights. Separation of each eye's ON and OFF cells into separate layers is for illustrative purposes only. The correlation function $C^{\mathrm{RN,LN}}(\vec{\alpha}, \vec{\beta})$ measures the degree of correlation between the spiking activities of LGN neurons of type RN (right-eye, ON-center) at position $\vec{\alpha}$, and those of type LN (left-eye, ON-center) at position $\vec{\beta}$. In principle there are ten such correlation functions, representing the correlations between each pair of LGN cell types drawn from $\{RN,RF,LN,LF\}$. The intra-cortical interaction function $I(\vec{x}, \vec{y})$ describes how activity at cortical location $\vec{x}$ encourages or discourages the development of correlated synaptic connections at a nearby location $\vec{y}$.

Figure 2. Within-eye correlation functions used during monocular deprivation and reverse suture simulations (correlations between the eyes are set to zero). These functions are made from combinations of a spatially oscillating function M (a), and a broad non-oscillating function G_3 (b). (c,d) Correlation functions used within a non-deprived eye ($N_{\mathcal{E}}$) are set to functions that can be written as the sum of (1) the spatially oscillating function M, with opposite signs for same center-type ($S_{\mathcal{C}}$) vs. opposite center-type ($O_{\mathcal{C}}$) inputs; and (2) the broad function G_3, with identical sign for $S_{\mathcal{C}}$ and $O_{\mathcal{C}}$, and with strength proportional to a constant d. (c) $d=2$. (d) $d=6$. (e,f) Correlations within a deprived eye ($D_{\mathcal{E}}$) are simulated in two possible forms. (e) To simulate deprivation with TTX, the correlations are set to zero. (f) To simulate deprivation through eyelid suture, we set correlations proportional to G_3, positive for $S_{\mathcal{C}}$ and negative for $O_{\mathcal{C}}$, to represent the correlations that would be expected to occur due to light transmission through the closed eyelids.

Figure 3. Left-eye and right-eye orientation maps from several stages of a deprivation-and-reverse-suture simulation. Maps of orientation preference measured monocularly through each eye. White lines show orientations of the 32 by 32 cortical cells, with line lengths corresponding to orientation specificity. The underlying 64 by 64 pixel color maps are each obtained by linear interpolation of the corresponding 32 by 32 map. Here hue represents preferred orientation and brightness represents the total strength of input to each cortical location from LGN cells in one eye. The white square indicates the locations of receptive fields illustrated in Fig. 4. (row A) Initial conditions at onset of deprivation: weakly developed, binocularly correlated orientation maps without ocular dominance segregation. Correlation coefficient between the two eyes' orientation maps is 0.71. (row B) Conditions following monocular deprivation of the right eye, beginning from the initial state illustrated in row A. Correlation functions were as in Fig. 2c ($d = 2$), for the open eye, and as in Fig. 2f (Eyelid Suture) for the deprived eye. Deprivation continued until $\langle m \rangle \geq 0.60$, *i.e.* the mean strength of synaptic inputs from the closed, right eye had decreased to 40% of its value in row A. (row C) Conditions following simulated reverse suture. Beginning from the deprived state in row B, the previously-open left eye was deprived and the previously-closed right eye was opened. Development was continued until $\langle m \rangle \leq -0.60$, *i.e.* the mean strength of connections from the left eye had decreased to 40% of its value in row A, prior to initial deprivation. Open and closed eye correlation functions were as in row B, with open and closed eyes switched. After the initial deprivation, the cortex gives little activity in response to right-eye stimulation, but gives robust, orientation-selective responses to left-eye stimulation at most locations; the reverse is true after reverse suture. The orientation map measured through the right eye after reverse suture (row C) closely resembles the map obtained through the left eye after the initial monocular deprivation (row B). The correlation coefficient (see Methods) between these two maps is 79.5%. Parameters: $t_1 = 26$, eyelid suture, $d = 2$.

Figure 4. Change, with deprivation and reverse suture, in the receptive fields of the set of 8×8 cells with locations indicated by the white boxes in Fig. 3 (same simulation as in Fig. 3). In each row, the left two columns show left-eye and right-eye receptive fields, respectively, with brightness indicating synaptic strength on an absolute scale; the right two columns

repeat the left-eye and right-eye receptive fields but this time with brightness separately normalized in each 8×8 image to use the full dynamic range, so that the structure of even very weak synapses can be seen. In each receptive field, ON synaptic strength is shown as red and OFF synaptic strength as green, so that equal ON and OFF strength is shown as yellow. The top row shows the initial condition at the onset of deprivation; the middle row, the receptive fields after the initial deprivation; and the bottom row, the receptive fields after the reverse suture. After 60% deprivation, the right eye has very little synaptic strength (middle row, second column) and that which remains is noisy and irregular (middle row, fourth column), yet the map is largely restored after reverse deprivation.

Figure 5. Correlation coefficient between orientation maps in the initially deprived eye after initial deprivation and in the newly deprived eye after reverse suture, across multiple parameters. Top: correlation coefficient is plotted vs. percent deprivation, that is, the percentage of synaptic strength lost in the initially deprived eye. Bottom: correlation coefficient is plotted against the percentage of deprived-eye synapses that reached zero strength during the initial deprivation. After initial condition develops for indicated number of time steps (t_1) (as in the top row of Figs. 3-4), first monocular deprivation (as in middle row of Figs. 3-4), then reverse suture (as in bottom row of Figs. 3-4) each proceed until total strength projected by deprived eye is reduced by the given percentage, relative to its strength in the initial condition prior to the initial deprivation. Thus, 0% deprivation means development stops at the initial condition; while 60% deprivation means initial deprivation proceeds until deprived eye projects only 40% of its normal strength, and then reverse suture proceeds until newly deprived eye projects only 40% of its normal strength. The y-axis indicates correlation coefficient, r, between orientation map in initially open eye after initial deprivation, and orientation map in newly opened eye after reverse suture. A dotted line at correlation value 0.75 is provided to assist comparison of simulation results to the experimentally measured coefficients of 0.75-0.9 (Gödecke & Bonhoeffer, 1996). Depending on parameters, from 60 to 90% of deprived-eye synaptic strength can be lost without reducing correlation beyond this range. The more strongly developed the initial condition, the more synapses that were entirely lost in the initial deprivation (increasing t_1 represents increasingly strong develop-

ment of orientation maps before the onset of deprivation). Correlation functions used are described by "TTX" or "Non-TTX" (deprived eye) and value of d (open eye), Fig. 2. Note that, for small t_1, interocular correlation continues to rise after the onset of deprivation, although the two eyes' maps are developing completely independently; reasons are discussed in the Results. The "Non-TTX" simulations tend to de-correlate left- and right-eye maps more quickly than "TTX" simulations; this is because the broad Gaussian-correlated activity more quickly degrades the orientation specificity in the closed eye. We use values of d that allow ocular dominance segregation to develop when normal development is simulated in stage 2 (meaning both eyes have the activity patterns given the open eye during deprivation), because we assume deprivation does not alter activities in the open-eye inputs. This requires larger d for larger t_1 (for larger t_1, the orientation map is more fully developed and synapses are closer to saturation before ocular dominance begins to develop, so ocular dominance can emerge only if it develops more quickly). To check dependence on the random seed used to develop the initial map, we ran a total of ten monocular deprivation/reverse suture simulations with different random seeds for $t_1 = 66$, TTX, deprivation to loss of 80% of synaptic strength. The correlation coefficients from all ten simulations had a mean of 77.6% with a standard deviation of 4.0%.

Figure 6. Orientation maps from a simulation in which deprivation was modelled as random synapse deletion rather than as gradual change in synaptic strength. Conventions as in Fig. 3. Parameters: Random synapse deletion, $t_1 = 46$, eyelid suture, $d = 4$.

Figure 7. Receptive fields from the simulation of Fig. 6, from the cells indicated by the white squares in that figure. Conventions as in Fig. 4. Parameters: Random synapse deletion, $t_1 = 46$, eyelid suture, $d = 4$.

Figure 8. Correlation coefficient between orientation maps in the initially deprived eye after initial deprivation and in the newly deprived eye after reverse suture, vs. percent deprivation, across multiple parameters, for simulations in which deprivation was modelled as random deletion of deprived-eye synapses rather than as gradual loss of synaptic strength.

Conventions as in Fig. 5. If initial maps are well correlated, 60-80% of synaptic strength can be lost to random pruning without disrupting map correlation. However, random synaptic pruning destroys map correlation for $t_1 = 26$, when the initial condition (shown in Figs. 3-4, top) had only weak development of maps and receptive fields, with little ON/OFF segregation and only 71% correlation between the two eyes' maps.

Figure 1

(Print as a one-column figure.)

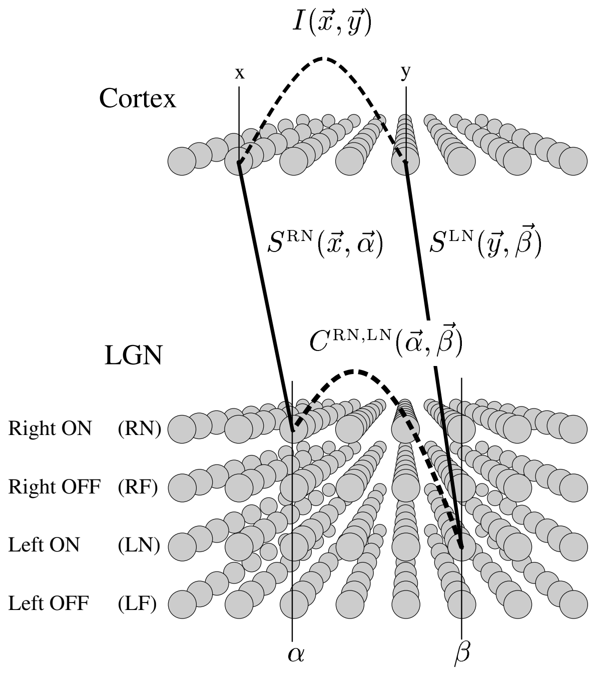

Figure 2

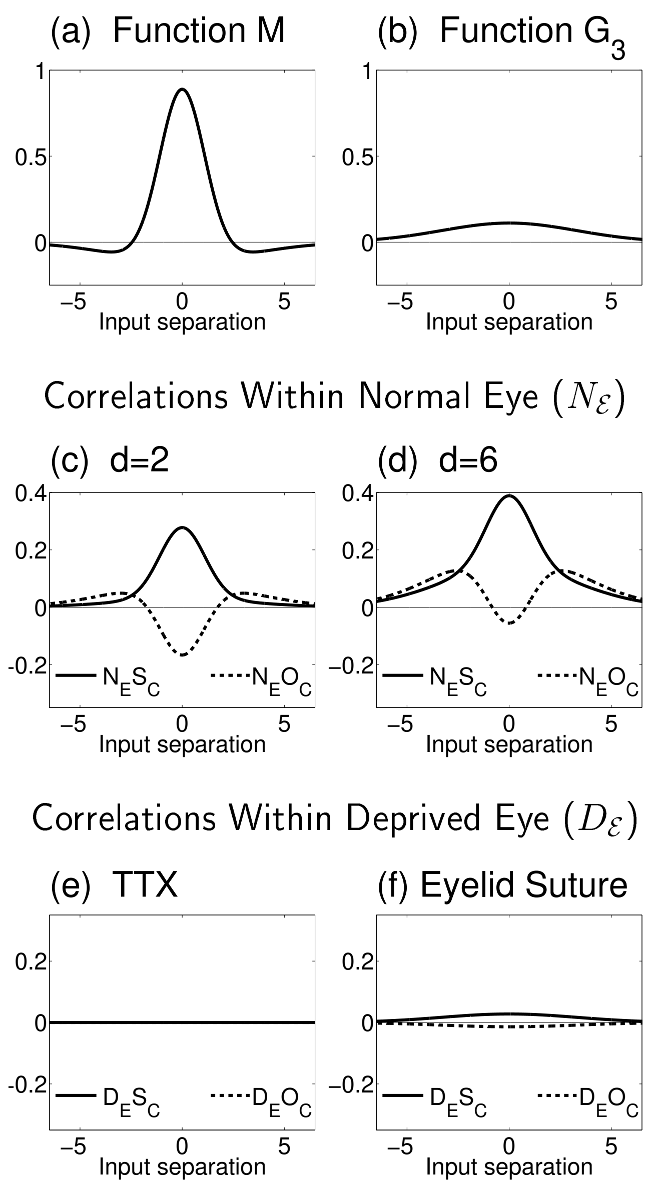
(a) Function M
(b) Function G_3
1
0.5
0
−5
5
Input separation
Correlations Within Normal Eye ($N_{\mathcal{E}}$)
(c) d=2
(d) d=6
0.4
0.2
-0.2
$N_E S_C$
$N_E O_C$
Correlations Within Deprived Eye ($D_{\mathcal{E}}$)
(e) TTX
(f) Eyelid Suture
$D_E S_C$
$D_E O_C$

Figure 3

(A) Initial Condition ($t_1 = 26$)

(B) After Initial Suture (until $\langle m \rangle = +0.60$)

(C) After Reverse Suture (until $\langle m \rangle = -0.60$)

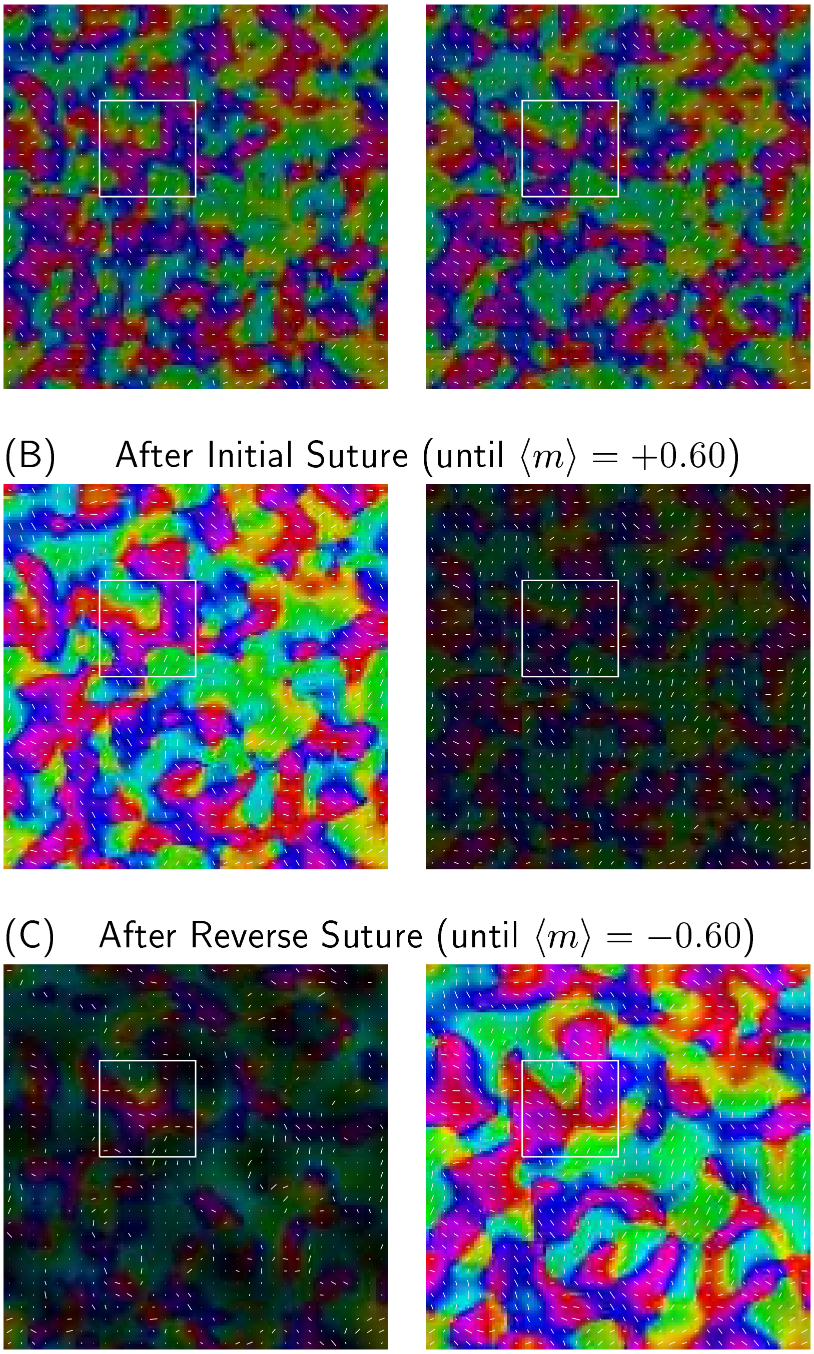

Left-eye ORI maps Right-eye ORI maps

Figure 4

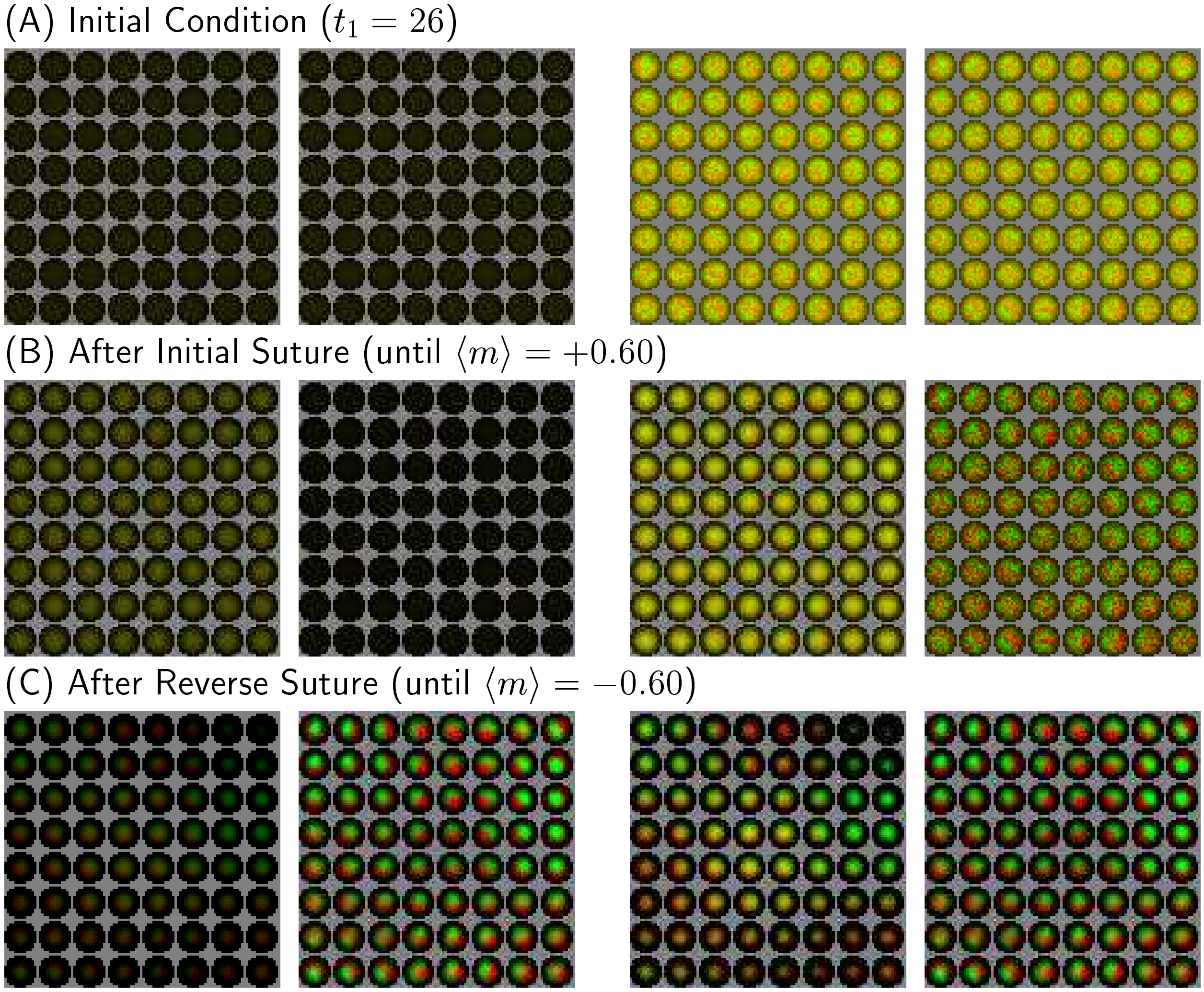
(A) Initial Condition ($t_1 = 26$)
(B) After Initial Suture (until $\langle m \rangle = +0.60$)
(C) After Reverse Suture (until $\langle m \rangle = -0.60$)

Figure 5

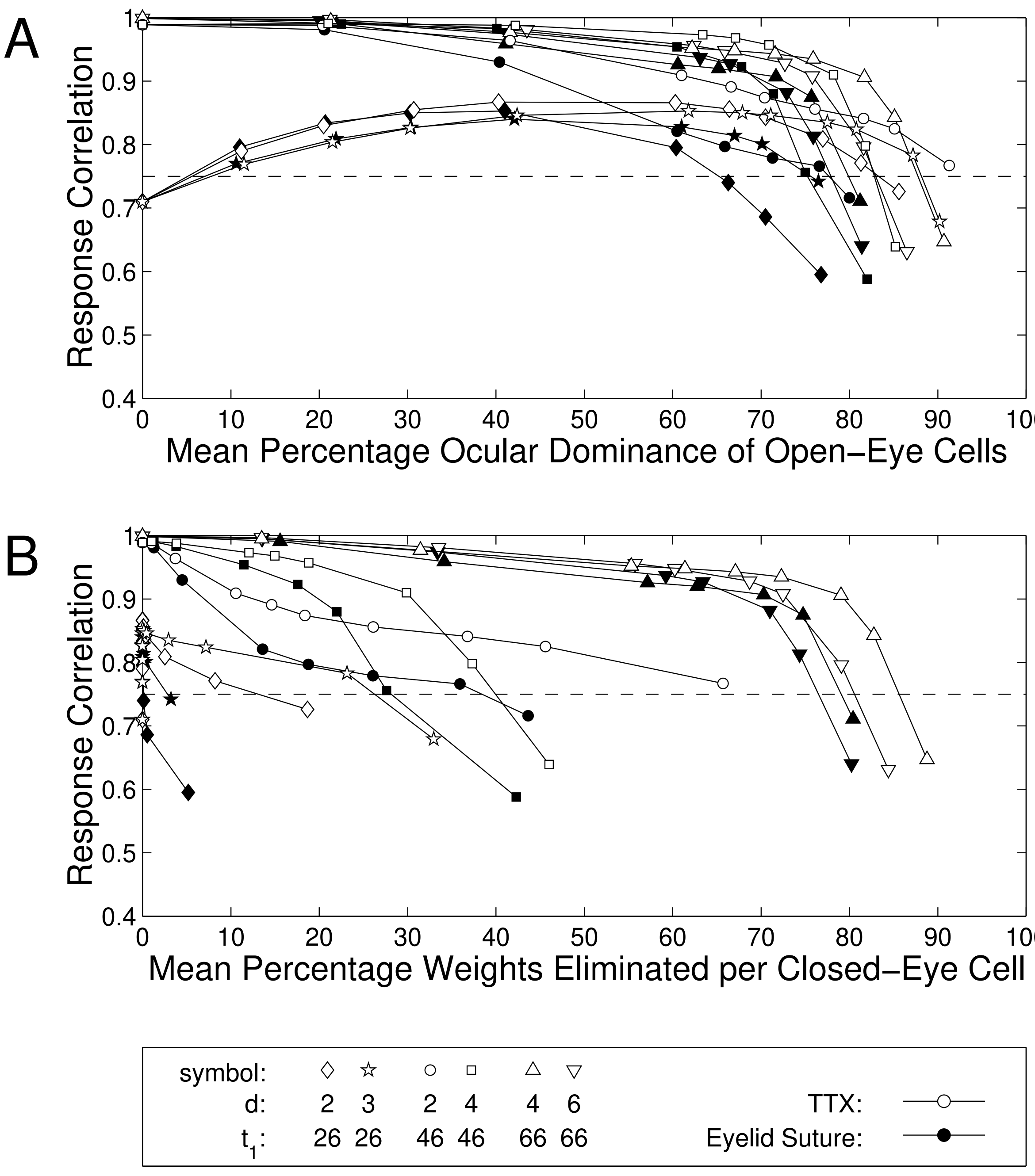
A
Response Correlation
Mean Percentage Ocular Dominance of Open−Eye Cells
B
Response Correlation
Mean Percentage Weights Eliminated per Closed−Eye Cell
symbol:
d: 2 3 2 4 4 6
t1: 26 26 46 46 66 66
TTX:
Eyelid Suture:

Figure 6

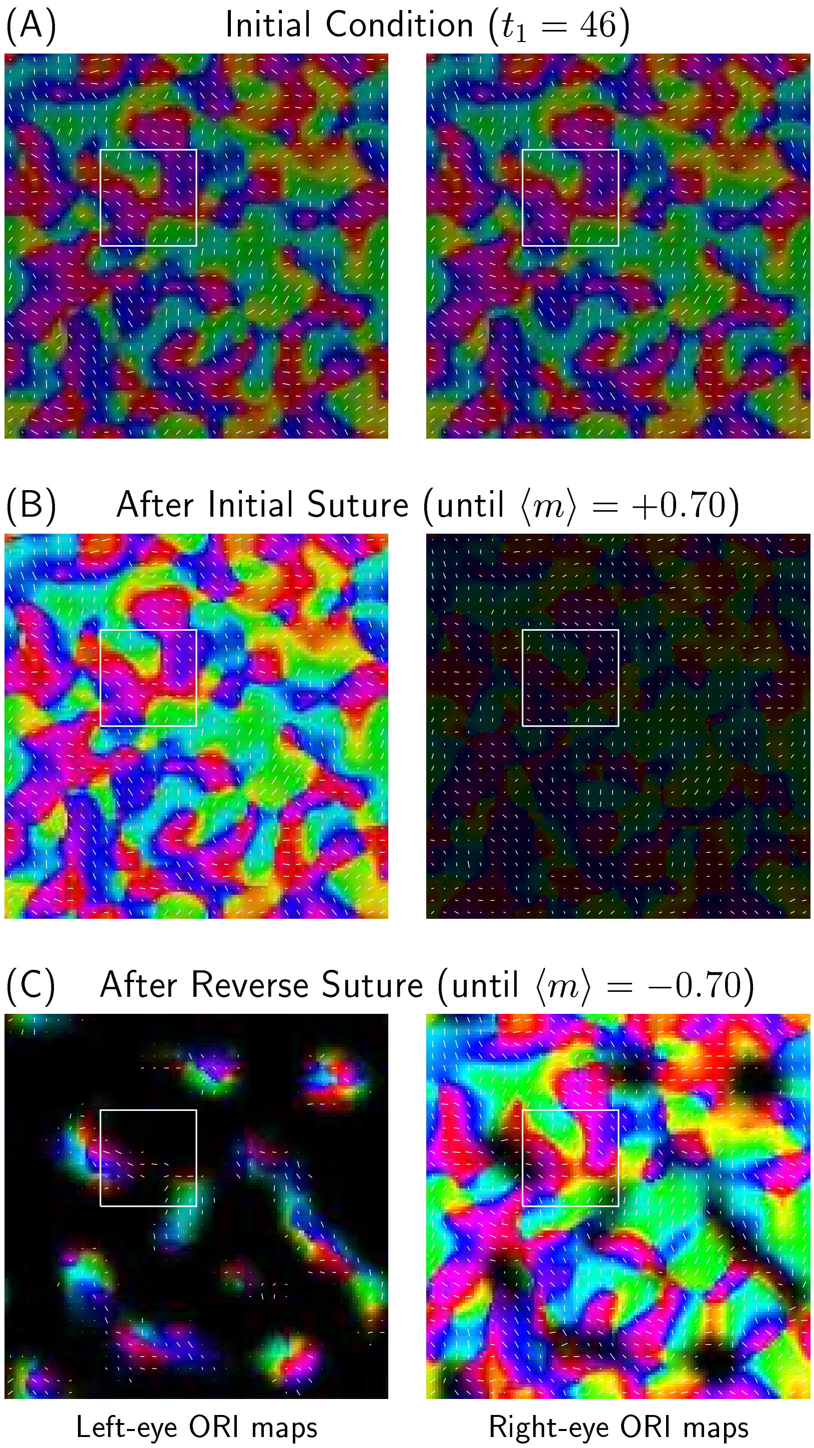
(A) Initial Condition ($t_1 = 46$)
(B) After Initial Suture (until $\langle m \rangle = +0.70$)
(C) After Reverse Suture (until $\langle m \rangle = -0.70$)
Left-eye ORI maps
Right-eye ORI maps

Figure 7

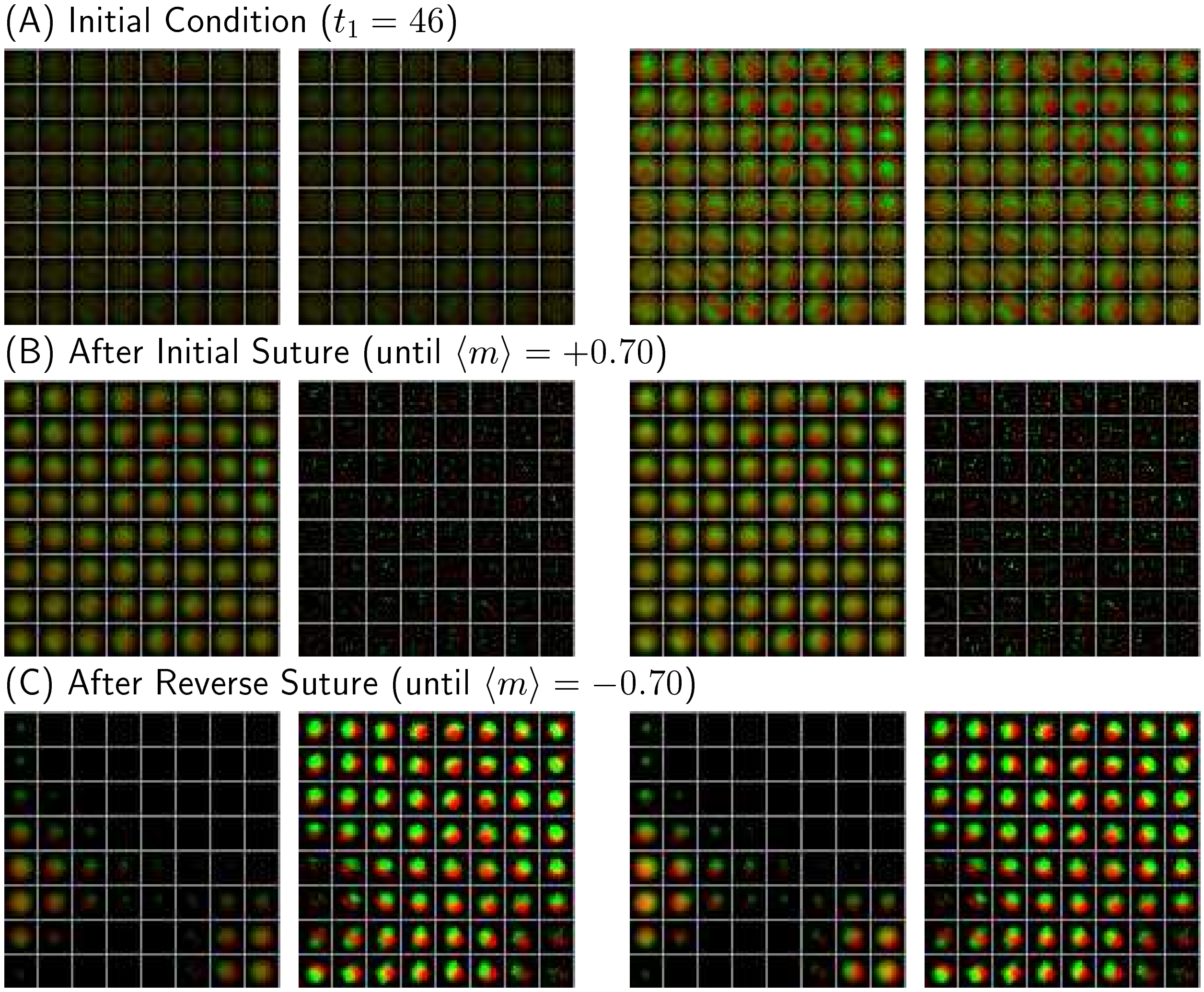
(A) Initial Condition ($t_1 = 46$)
(B) After Initial Suture (until $\langle m \rangle = +0.70$)
(C) After Reverse Suture (until $\langle m \rangle = -0.70$)

Figure 8

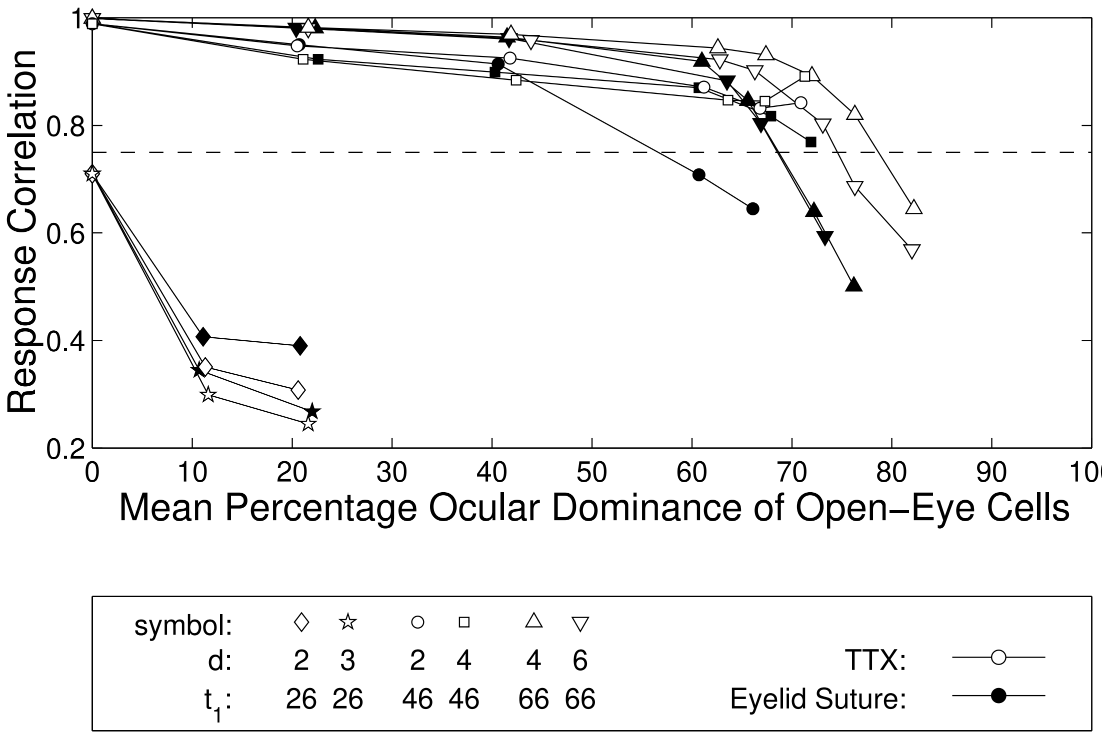

Response Correlation
Mean Percentage Ocular Dominance of Open−Eye Cells
0.2
0.4
0.6
0.8
1
0
10
20
30
40
50
60
70
80
90
100
symbol:
d: 2 3 2 4 4 6
t_1: 26 26 46 46 66 66
TTX:
Eyelid Suture: